13th Australia New Zealand Conference on Geomechanics – Acosta-Martínez & Lehane (Eds.)

An elasto-plastic constitutive model for the analysis of bonded geomaterials

H. Moghaddasi, M. Khoshini, A. Khoshghalb, N. Khalili
School of Civil and Environmental Engineering, UNSW Australia, NSW 2052, Australia

ABSTRACT: A constitutive model is proposed to simulate the behaviour of bonded geomaterials. The bounding surface plasticity framework with a non-associated flow rule is adopted and extended to account for the strength degradation due to the breakage of inter-particle bonds. The effects of the inter-particle bonds on the compressive and tensile strength of geomaterials are considered through the bounding surface and dilatancy law of the proposed model. A plastic cementation index is included in the model to capture the degradation process by controlling the size of the bounding surface. The destruction of the bonds is included in the hardening modules allowing for a smooth transition of the response from bonded to unbonded states. The model can simulate the volume change behaviour and softening response of both reconstituted and bonded geomaterials. To demonstrate the capability of the model, several laboratory tests are simulated, and their corresponding results are compared with the measured experimental data.

1 INTRODUCTION

For porous media without inter-particle bonds, the initial porosity and applied stress are the main state variables for tracing and predicting the mechanical behaviour. In the presence of inter-particle bonds, however, the material can withstand a relatively higher pressure before exhibiting bond breakage and strength degradation behaviour (Leroueil & Vaughan 1990). Quantification of the effect of such inter-particle bonds and the associated destruction rate is of particular importance in evaluating the strength of bonded geomaterials.

Bonded geomaterials cover a large area of shallow stratum, which includes cemented soils, weak rocks and structural soils. The phenomenological constitutive models based on the theory of plasticity has gained noticeable attention for predicting the behaviour of the bonded geomaterials. In the classical theory of plasticity, the effect of inter-particle bonding is portrayed through the enlargement of the yield surface (Muir Wood 1995, Liu & Carter 2002, Asaoka et al. 2000) and inclusion of a tensile strength (Gens 1993, Lagioia & Nova 1995, Rouainia & Muir Wood 2000, Yu et al. 2007, Yan & Li 2010, Nova et al. 2003, Kavvadas & Amorosi 2000). The destruction process in these models are triggered either by the accumulation of the plastic strain (Lagioia & Nova 1995, Asaoka et al. 2000, Rouainia & Muir Wood 2000, Kavvadas & Amorosi 2000, Yu et al. 2007, Yan & Li 2010) or attainment of a specified stress level (Liu & Carter 2002, Horpibulsuk et al. 2010, Nguyen et al. 2014), while few models incorporated simultaneous effect of the stress and strain tensors in degradation phenomenon (Lade & Kim 1995, Yasin & Tatsuoka 2000). The conventional elasto-plastic framework with a single yield surface have been typically adopted for the constitutive modellings of bonded geomaterials, rendering them unable to capture debonding process below the yield level. To address this shortcoming, a few models based on the bounding surface plasticity framework have been, so far, proposed to predict the destruction phenomenon in geomaterials (Suebsuk et al., Liu 2010, Chen et al. 2014). However, these models are based on the assumption that bond degradation is triggered at some threshold plastic strain or stress magnitude, while it has been noted that in fact, the simultaneous effects of state variables result in the destruction process (Lade 1995, Xiao et al. 2016).

This paper presents an advanced plasticity model based on the bounding surface plasticity framework to simulate the behaviour of bonded geomaterials. The strength increase in the materials due to the presence of the inter-particle bonds is captured by adjusting the size of the bounding and plastic potential surfaces. The evolution of these surfaces is linked to the accumulation of the plastic volumetric strain and a cementation index describing the irreversible destruction process. The model reduces to

the bounding surface plasticity model previously proposed for unbounded materials (Khalili et al. 2005, Kan et al. 2014) when the strength effects of the bonds vanish. The performance of the model is demonstrated through the simulation of a set of experimental data from the literature.

2 THE BOUNDING, LOADING AND PLASTIC POTENTIAL SURFACES

The locus of all possible stress states in a material is enclosed by a bounding surface on which the behavior of the material is dominantly plastic. In the bounding surface plasticity formulation, the distance between the stress point, $\boldsymbol{\sigma}'$, and an image point on the bounding surface, $\bar{\boldsymbol{\sigma}}'$, is exploited to obtain the hardening modules. In unbonded geomaterials, the shape of the bounding surface can be estimated from their undrained response in the loosest state. For bonded geomaterials, the shape of the bounding surface should, however, account for the additional compressive and tensile strengths due to the presence of the bonds. According to the bounding surface plasticity framework, the current stress state should always lie on a loading surface which is homologous to the bounding surface about a centre of homology. To fulfil this requirement, a shape similar to the one assumed for the bounding surface, is selected for the loading surface. The stress point corresponding to tensile strength of the material is selected as the centre of homology, and the radial mapping rule is performed to locate an image point on the bounding surface, as depicted in Figure 1a. The following analytical functions are assumed for the loading and bounding surfaces

$$F(\bar{p}'^{*},\bar{q},\bar{\theta},\bar{p}'_c)=\left(\frac{\bar{q}}{M_{cs}(\bar{\theta})\bar{p}'^{*}}\right)^{N}-\frac{ln\left(\bar{p}'_c/\bar{p}'^{*}\right)}{ln(R)}=0 \tag{1}$$

$$f\left(p'^{*},q,\theta,p'_c\right)=\left[\frac{q}{M_{cs}(\theta).p'^{*}}\right]^{N}-\frac{ln\left(p'_c/p'^{*}\right)}{ln(R)}=0 \tag{2}$$

where p'^{*}, q and θ are the modified mean effective stress, deviatoric stress and Lode angle, respectively. $\bar{p}'^{*}, \bar{q}$ and $\bar{\theta}$ are the similar quantities at the image point on the bounding surface. N and R are two material parameters controlling the shape of the loading and bounding surfaces. $\bar{p}'_c$ is the hardening parameter. The modified mean effective stresses and hardening parameter are defined as follows,

$$\begin{aligned}\bar{p}'^{*}&=\bar{p}'+\bar{p}'_t\\ p'^{*}&=p'+\bar{p}'_t\\ \bar{p}'_c&=\bar{p}'_t+\bar{p}'_s+\bar{p}'_m\end{aligned} \tag{3}$$

where $\bar{p}'_s$ is the strength variable representing the contribution of the fully debonded material, while $\bar{p}'_t$ and $\bar{p}'_m$ are the strength variables associated with the effect of inter-granular bonds, as depicted in Figure 1b. $M_{cs}(\bar{\theta})$ is the slope of the critical state line (CSL) in the stress space defined as (Sheng et al. 2000)

$$M_{cs}(\bar{\theta})=M_{max}\left[\frac{2\alpha^4}{1+\alpha^4-(1-\alpha^4)\sin(3\bar{\theta})}\right]^{1/4} \tag{4}$$

in which $\alpha=M_{max}/M_{min}$ with M_{max} and M_{min} being the slope of the CSL at triaxial compression and extension, respectively. The slope of the CSL in extension is linked to its corresponding slope in compression through $M_{min}=3M_{max}/(M_{max}+3)$. If the strength parameters associated with inter-particle bonds are vanished, the destructed bounding surface is obtained (see Figure 1b).

To characterize the volume change behaviour of bonded geomaterials, a generalized form of the Row's dilatancy law including the effect of tensile strength of the bonded materials is proposed

$$d=\frac{\Delta\varepsilon_p^p}{\Delta\varepsilon_q^p}=A\left(M_{cs}(\theta)-\frac{q}{p'^{*}}\right) \tag{5}$$

where d is the dilatancy, $\Delta\varepsilon_p^p$ and $\Delta\varepsilon_q^p$ are the rates of volumetric and deviatoric strains, respectively, and A is a material parameter. By integrating the dilatancy law with respect to stress, the plastic potential function is obtained,

$$\begin{aligned}&g(p'^{*},q,\theta,p'_0)=q+M_{cs}(\theta)p'^{*}\ln\left(p'^{*}/p'_0\right)\\ &\text{for A=0}\\ &g(p'^{*},q,\theta,p'_0)=q+\frac{AM_{cs}(\theta)p'^{*}}{A-1}\left(\left(\frac{p'^{*}}{p'_0}\right)^{A-1}-1\right)\\ &\text{for A}\neq 0\end{aligned} \tag{6}$$

where p_0 is a dummy parameter since only the derivates of g appear in the model.

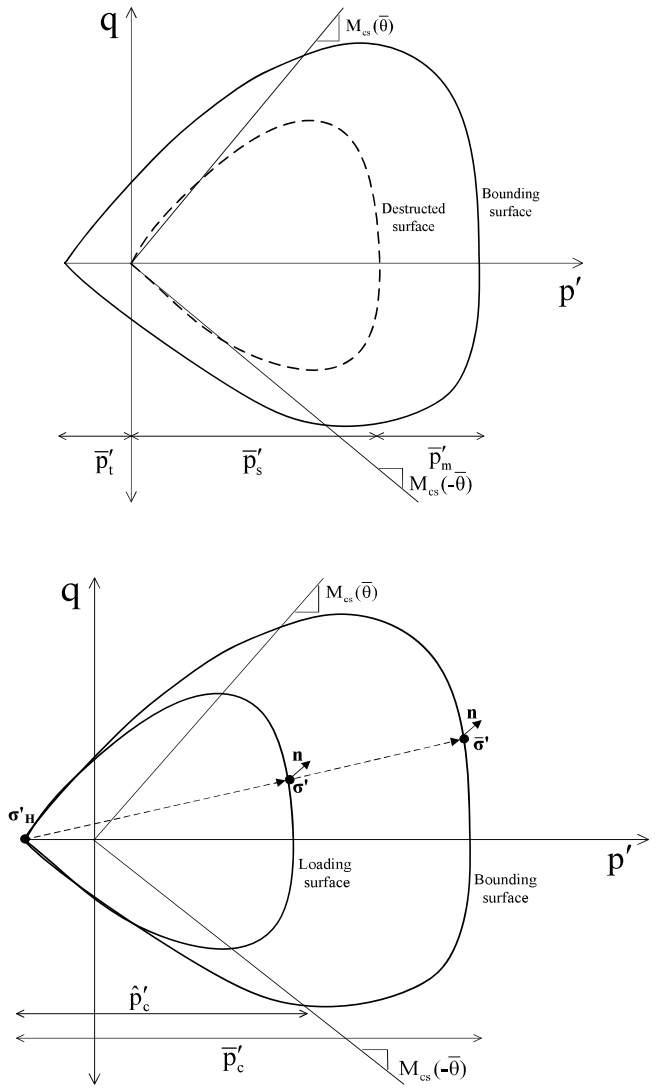

Figure 1. a) The bounding surface and loading surface for bonded geomaterials; b) the contribution of various strength parameters in the shape of the bounding surface.

3 THE EVOLUTION OF CHARACTERISTIC SURFACES

The size of the bounding surface is defined as a function of the hardening parameter. For bonded geomaterials, the evolution of the hardening parameter is associated with the variation of both plastic volumetric strain ε_p^p and a plastic cementation index I_c. The latter accounts for the contribution of the interparticle bonds, while the former includes the effects of frictional contacts between grains. On the bounding surface, the consistency condition can be written as

$$dF(\bar{\boldsymbol{\sigma}}', \bar{p}'_c(\varepsilon_p^p, I_c)) = \left(\frac{\partial F}{\partial \bar{\boldsymbol{\sigma}}'}\right)^T \Delta\bar{\boldsymbol{\sigma}}' + \frac{\partial F}{\partial \bar{p}'_c}\frac{\partial \bar{p}'_c}{\partial \varepsilon_p^p}\Delta\varepsilon_p^p + \frac{\partial F}{\partial \bar{p}'_c}\frac{\partial \bar{p}'_c}{\partial I_c} dI_c = 0 \quad (7)$$

It is assumed that destruction of the bonds occurs by the increase of the stress magnitude and accumulation of the plastic strain, which can be quantified by an index related to the plastic work. Therefore, the following relation is proposed for the rate of the plastic cementation index

$$dI_c = \rho_c(1 - I_c)(dw^p / p'_1) \quad (8)$$

where ρ_c is a dimensionless positive material parameter controlling the rate of strength degradation in bonded geomaterials, p'_1 is a reference pressure and dw^p is the increment of plastic work expressed as

$$dw^p = \left|p'\Delta\varepsilon_p^p\right| + \left|q\Delta\varepsilon_q^p\right| \quad (9)$$

Integrating equation (8) with respect to the plastic work shows that I_c is zero for the bonded materials before any destruction occurs, and it reaches a unit value once all the bonds are broken. The response of the bonded material subject to isotropic loading can determine the evolution of $\bar{p}'_s$ and $\bar{p}'_m$, and therefore the hardening parameter. According to the critical state soil mechanics, the response of the fully debonded material follows a straight line (LICL) in $\upsilon - \ln p'$ where υ is the specific volume at the current stress. This line, which can be quantified by the intersection at the reference pressure of 1 kPa, N_{LICL}, and the slope λ, serves as the ultimate state of the bonded material when all the bonds are destructed. To this end, evolutions of strength variables ($\bar{p}'_s$, $\bar{p}'_m$ and $\bar{p}'_t$) with respect to I_c and ε_p^p are assumed as follows,

$$\frac{\partial \bar{p}'_m}{\partial I_c} = \frac{-\bar{p}'_m}{(1 - I_c)}, \frac{\partial \bar{p}'_t}{\partial I_c} = \frac{-\bar{p}'_t}{(1 - I_c)} \text{ and } \frac{\partial \bar{p}'_s}{\partial \varepsilon_p^p} = \frac{\upsilon \bar{p}'_s}{\lambda - \kappa} \quad (10)$$

where κ is the slope of unloading-reloading curve in the $\upsilon - \ln p'$ plane. Substituting equations (8) to (10) in the consistency condition (equation (7)) and utilizing equation (5), the hardening modules on the bounding surface can be obtained as,

$$h_b = \bar{h}_t + \bar{h}_s + \bar{h}_m \tag{11}$$

in which

$$\bar{h}_t = \frac{1}{\left\|\partial F/\partial \bar{\boldsymbol{\sigma}}'\right\|}\frac{\partial F}{\partial \bar{p}_t'}\left(\frac{\rho_c \bar{p}_t'}{p_1'}\left(\left|p' m_p\right| + \left|q m_q\right|\right)\right) \tag{12}$$

$$\bar{h}_s = -\frac{1}{\left\|\partial F/\partial \bar{\boldsymbol{\sigma}}'\right\|}\frac{\partial F}{\partial \bar{p}_s'}\left(\frac{\upsilon \bar{p}_s'}{\lambda - \kappa} m_p\right) \tag{13}$$

$$\bar{h}_m = \frac{1}{\left\|\partial F/\partial \bar{\boldsymbol{\sigma}}'\right\|}\frac{\partial F}{\partial \bar{p}_m'}\left(\frac{\rho_c \bar{p}_m'}{p_1'}\left(\left|p' m_p\right| + \left|q m_q\right|\right)\right) \tag{14}$$

with

$$m_p = \frac{\partial g/\partial p'^*}{\left\|\partial g/\partial \boldsymbol{\sigma}'\right\|}, \quad m_q = \frac{\partial g/\partial q}{\left\|\partial g/\partial \boldsymbol{\sigma}'\right\|} \tag{15}$$

In accordance with the usual approach in the bounding surface plasticity, the plastic hardening module is assumed to comprise two terms

$$h = h_b + h_f \tag{16}$$

h_f is the hardening modulus at the current stress point, which is required to be zero on the bounding surface and infinity at the centre of homology. In the current study, the following analytical function is assumed for h_f,

$$h_f = \frac{\upsilon p'^*}{(\lambda - \kappa)}\left[\frac{\bar{p}_c'}{p_c'} - 1\right] k_m (\eta_p - \eta) \tag{17}$$

where $\eta = q / p'^*$ is the stress ratio and $\eta_p = \left(1 - 2(\upsilon - \upsilon_{cs})\right) M_{cs}(\theta)\, \bar{p}_c' / \bar{p}_s'$ is the slope of peak strength line. k_m is a material parameter controlling the hardening modulus and υ_{cs} is the specific volume on the CSL corresponding to the current state. The CSL line is defined parallel to the LICL with a constant shift in $\upsilon - \ln p'$ plane along the recompression line. The intersection of the CSL at the reference pressure of 1 kPa is denoted by Γ.

To obtain the elasto-plastic stiffness tensor, elastic behaviour of the material must also be included. In this study, a bond-independent elastic behaviour is assumed through the following bulk and shear modulus,

$$K = \frac{\upsilon p'}{\kappa} \tag{18}$$

$$G = \frac{3(1-2\nu)}{2(1-\nu)}\frac{\upsilon p'}{\kappa} \tag{19}$$

where ν is the Poisson's ratio.

4 MODEL EVALUATION

Burland et al. (1996) conducted a series of conventional laboratory tests on stiff Pietrafitta clay to investigate its elastoplastic behaviour. Both intact and reconstituted samples of Pietrafitta clay were tested in oedometer and triaxial apparatus, in both drained and undrained conditions, to investigate the effect of micro-structure on the response of the natural clay. The basic material parameters of the model, including those related to the LICL and CSL in the stress space, are found based on the response of the reconstituted material. Typical values are adopted for the parameters related to the elastic properties of the clay. The parameters related to the bond's strength are determined by comparing the yield surfaces of the intact and reconstituted clays obtained in triaxial tests. The complete list of the material parameters adopted in the simulations are given in Table 1.

Table 1. The mechanical properties of Pietrafitta clay

κ	ν	M_{max}	N
0.031	0.25	1.13	4

R	A	k_m	λ
3	2	4	0.227

Γ	p_m (kPa)	p_t (kPa)	ρ_c
3.295	900	50	0.004

The simulated and measured responses of the intact Pietrafitta clay in oedometer test are depicted in Figure 2a. It is seen from the results that the initial structure of the natural clay breaks as the stress increases, and the response of the reconstituted sample can be recovered at a large vertical stress. As can be seen from Figure 2a, the model proposed in this study satisfactorily represents the experimental results.

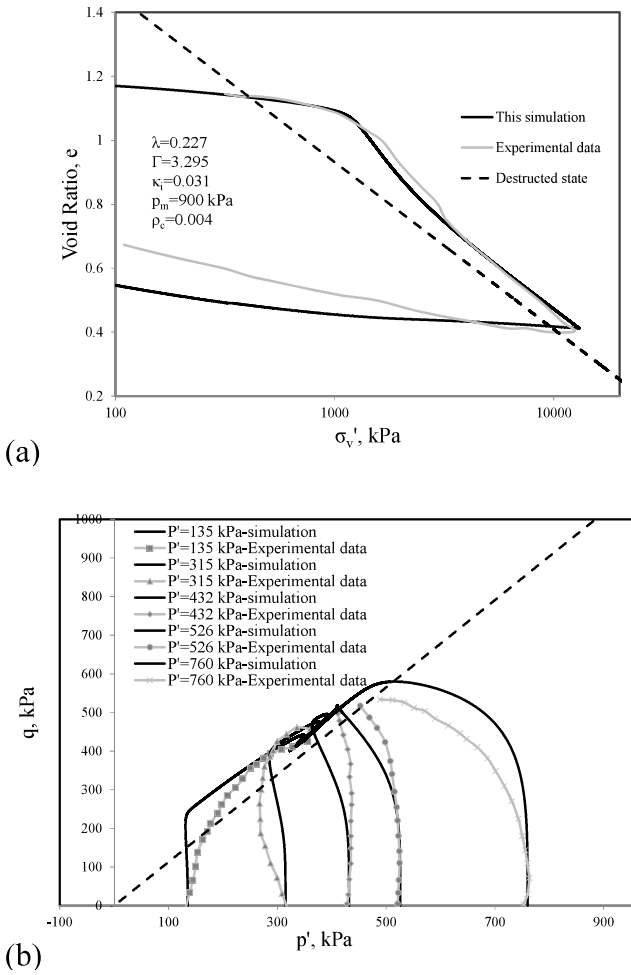

Figure 2. The predicated and measured behaviour of Pietrafitta clay subject to a) one-dimensional consolidation test, b) undrained triaxial tests.

The response of the Pietrafitta clay under undrained triaxial tests is also studied. A number of saturated clay samples with various effective confining pressures were prepared and tested in triaxial tests by Burland et al. (1996). The effective stress path obtained from the experiment data along with the corresponding simulations are depicted in Figure 2b. From both experimental and simulated results, it is clear that compared to the ultimate strength predicted by the CSL, higher peak stresses are obtained for natural clays. The post-peak softening behaviour is mainly due to the breakage of inter-particle bonds. The stress-stain behaviour and pore water pressure change of the samples are shown in Figure 3. By increasing the confining pressure, increase in the shear strength of the clay samples was observed in the experiments and satisfactorily predicted by the model proposed. From the results of pore water pressure change with respect to axial strain, it is seen that the tendency of the sample for dilatant behaviour increases as the confining pressure decreases. This is represented by the reduction of pore water pressure in the experimental data as the confining stress decreases, which is satisfactorily captured in the model. The difference between the predicted and measured response can be attributed to the localized behavior observed in the experimental data at low confining pressures. Such localized behavior cannot be captured by the constitutive model implemented at the scale of a single element.

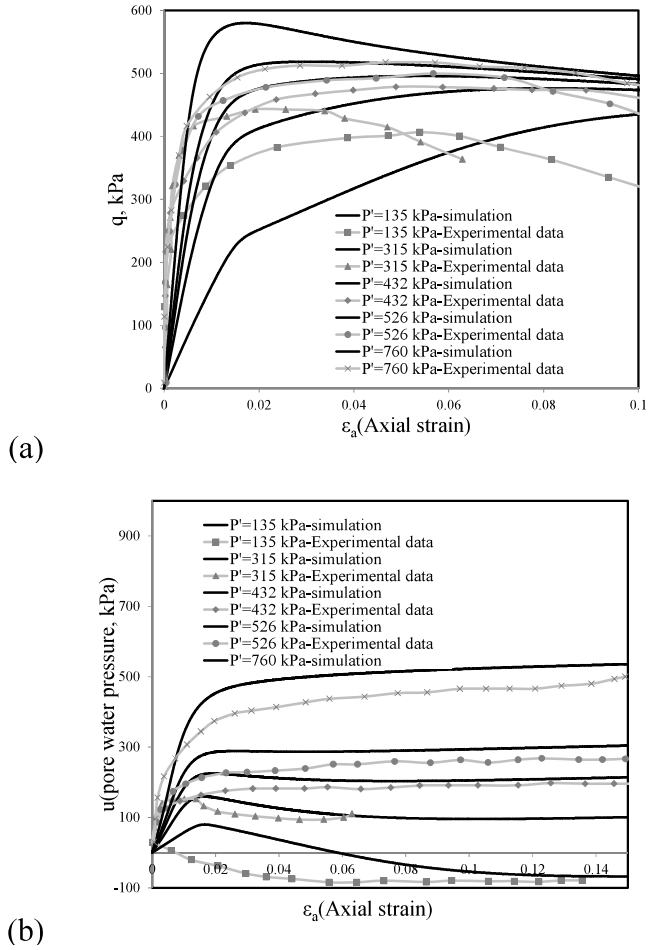

Figure 3. The predicated and measured behaviour of Pietrafitta clay obtained from undrained triaxial tests.

5 CONCLUSION

A constitutive model on the premise of the bounding surface plasticity formulation was proposed to simulate the response of the bonded geomaterials. The mathematical framework for predicting the response of the porous media was extended to include the effect of the inter-granular bonds and the destruction process due to loading. The extension was achieved through the modification of the yield surface and dilatancy law of unbonded materials. The softening behaviour of bonded geomaterials was captured in the hardening modules, which accounted for simultaneous effects of the stress magnitude and plastic strain in the debonding process. The response of several samples of stiff clays subject to both one-

dimensional compression and undrained shearing was simulated and compared to the experimental data. It was shown that the model can satisfactorily capture the increase in the strength of the stiff clays due to the bond effects, and the subsequent softening behaviour due to bond breakage. The undrained shear response of the clay samples under a range of confining pressures were also studied. It was shown that the proposed model can successfully predict the experimentally observed higher peak shear strengths in natural clay samples, compared to the reconstituted samples. The advantage of the proposed model is that it can capture a smooth bond breakage behavior by using reasonably low number of material parameters, all of which can be identified through standard laboratory tests.

REFERENCES

Asaoka, A., Nakano, M., & Noda, T. 2000. Superloading yield surface concept for highly structured soil behavior. *Soils and Foundations*, 40(2): 99-110.

Burland, J., Rampello, S., Georgiannou, V., & Calabresi, G. 1996. A laboratory study of the strength of four stiff clays. *Geotechnique*, 46(3): 491-514.

Chen, Q., Indraratna, B., Carter, J., & Rujikiatkamjorn, C. 2014. A theoretical and experimental study on the behaviour of lignosulfonate-treated sandy silt. *Computers and Geotechnics*, 61: 316-327.

Gens, A. 1993. Conceptual bases for a constitutive model for bonded soils and weak rocks. *Geotechnical engineering of hard soils-soft rocks*, 485-494.

Horpibulsuk, S., Liu, M. D., Liyanapathirana, D. S., & Suebsuk, J. 2010. Behaviour of cemented clay simulated via the theoretical framework of the structured cam clay model. *Computers and Geotechnics*, 37(1-2): 1-9.

Kan, M. E., Taiebat, H. A., & Khalili, N. 2014. Simplified mapping rule for bounding surface simulation of complex loading paths in granular materials. *International Journal of Geomechanics*, 14(2): 239-253. doi: 10.1061/(ASCE)GM.1943-5622.0000307

Kavvadas, M., & Amorosi, A. 2000. A constitutive model for structured soils. *Geotechnique*, 50(3), 263-273.

Khalili, N., Habte, M. A., & Valliappan, S. 2005. A bounding surface plasticity model for cyclic loading of granular soils. *International Journal for Numerical Methods in Engineering*, 63(14): 1939-1960. doi: 10.1002/nme.1351

Lade, P. V., & Kim, M. K. 1995. Single hardening constitutive model for soil, rock and concrete. *International Journal of Solids and Structures*, 32(14): 1963-1978.

Lagioia, R., & Nova, R. 1995. An experimental and theoretical study of the behaviour of a calcarenite in triaxial compression. *Geotechnique*, 45(4): 633-648.

Leroueil, S., & Vaughan, P. 1990. The general and congruent effects of structure in natural soils and weak rocks. *Geotechnique*, 40(3): 467-488.

Liu, M., & Carter, J. 2002. A structured Cam Clay model. *Canadian Geotechnical Journal*, 39(6): 1313-1332.

Muir Wood, D. 1995. Kinematic hardening model for structured soil. *Numerical Models in Geomechanics*, 83-88.

Nguyen, L. D., Fatahi, B., & Khabbaz, H. 2014. A constitutive model for cemented clays capturing cementation degradation. *International Journal of Plasticity*, 56: 1-18.

Nova, R., Castellanza, R., & Tamagnini, C. 2003. A constitutive model for bonded geomaterials subject to mechanical and/or chemical degradation. *International Journal for Numerical and Analytical Methods in Geomechanics*, 27(9): 705-732.

Rouainia, M., & Muir Wood, D. 2000. A kinematic hardening constitutive model for natural clays with loss of structure. *Geotechnique*, 50(2): 153-164.

Sheng, D., Sloan, S. W., & Yu, H. S. 2000. Aspects of finite element implementation of critical state models. *Computational mechanics*, 26(2), 185-196.

Suebsuk, J., Horpibulsuk, S., & Liu, M. D. 2010. Modified Structured Cam Clay: A generalised critical state model for destructured, naturally structured and artificially structured clays. *Computers and Geotechnics*, 37(7-8): 956-968.

Xiao, H., Lee, F. H., & Liu, Y. 2016. Bounding surface cam-clay model with cohesion for cement-admixed clay. *International Journal of Geomechanics*, 17(1): 04016026.

Yan, W., & Li, X. 2010. A model for natural soil with bonds. *Geotechnique*.

Yasin, S., & Tatsuoka, F. 2000. Stress history-dependent deformation characteristics of dense sand in plane strain. *Soils and Foundations*, 40(2): 77-98.

Yu, H., Tan, S., & Schnaid, F. 2007. A critical state framework for modelling bonded geomaterials. *Geomechanics and Geoengineering*, 2(1): 61-74.